Development of the Autonomous Mobile Overhead Traveling Crane in Consideration of On-line Obstacle Recognition, Path Planning and Oscillating Control

Y. Kawasaki, A. Kaneshige and S. Ueki
Toyota National College of Technology, Eisei-cho 2-1 Toyota-City, Aichi 471-8525, Japan

Keywords: Overhead Traveling Crane, Path Planning, Obstacle Recognition, Oscillating Control, Control Technology.

Abstract: In order to establish an autonomous overhead traveling crane system, it is needs to be constructed the obstacle recognition system, the path planning system and the control system of suppression of object swing automatically. These systems development is studied by our research group. In particular, the on-line obstacle recognition system using an ultrasonic sensor and the on-line obstacle avoidance path planning system of the on-line which extended the obstacle avoidance path planning method of the autonomous mobile robot which Srinivas has proposed to the three-dimensional obstacle avoidance path planning system are developed. Furthermore, the feed-forward control system using a notch filter is constructed. However, the feed-forward control system was not able to control object swing which occurred during initial deviation or transportation. Therefore, in order to improve the vibration suppression of object swing, 2-degrees of freedom control system is constructed in this research. It is unified with the obstacle recognition system and path planning system which are proposed until now, and the usefulness of the autonomous overhead traveling crane system integrated was confirmed.

1 INTRODUCTION

Development of an automation or an autonomous an overhead traveling crane are desired from viewpoint of working efficiency or safety. In order to establish an autonomous overhead traveling crane system, it is needs to be constructed the obstacle recognition system, the path planning system and the control system of suppression of object swing automatically. Especially, an obstacle recognition system and a path planning system that can be quickly carried out with an easy algorithm on-line are desired. These systems development is proposed by our research group (Kaneshige, 2012; Nagai,2011). In particular, the on-line obstacle recognition system using an ultrasonic sensor(USS) and the on-line obstacle avoidance path planning system which extended the obstacle avoidance path planning method of the autonomous mobile robot which Srinivas (Srinivas, 1991) has proposed to the three-dimensional obstacle avoidance path planning system are developed (Kaneshige, 2012; Nagai, 2011). In these proposed system, an obstacle avoidance path can be derived by information of target position and any obstacle position that is recognized by the obstacle recognition system. This on-line path plan method performs a path plan by the partial information of a transportation environment recognized by USS of the obstacle recognition system during transfer. The path plan of the overhead traveling crane is constructed to the goal position by repeating a suggested process (algorithm). And the usefulness of the proposed path planning method was evaluated from a view point of a qualitative and a quantitative (Nagai, 2011). On the other hand, the feed-forward control system using a notch filter is constructed (Kaneshige, 2012). However, the feed-forward control system was not able to control object swing which occurred during initial deviation or transportation.

Therefore, in order to improve the vibration suppression of object swing, two-degrees of freedom control system is constructed in this research. It is make to integrate in the obstacle recognition system and path planning system which is proposed previous researches, and the usefulness of the autonomous overhead traveling crane system integrated was confirmed.

Kawasaki Y., Kaneshige A. and Ueki S..
Development of the Autonomous Mobile Overhead Traveling Crane in Consideration of On-line Obstacle Recognition, Path Planning and Oscillating Control.
DOI: 10.5220/0005047103820389
In *Proceedings of the 11th International Conference on Informatics in Control, Automation and Robotics* (ICINCO-2014), pages 382-389
ISBN: 978-989-758-040-6
Copyright © 2014 SCITEPRESS (Science and Technology Publications, Lda.)

2 CONSTRUCTION OF EXPERIMENTAL EQUIPMENT AND OBSTACLE RECOGNITION SYSTEM

General view of the overhead traveling crane experimental equipment is shown in Fig.1. The experimental equipment is operated by servomotor attached in the X, Y, and Z-direction respectively. In the X-direction, the girder of crane is moved, in the Y-direction, the cart on the girder is moved, and in the Z-direction, a object is gone up and down, therefore, a object is transferred. The swing angle of X-direction(α) and Y-direction(β) is measured by the rotary encoder fixed to the cart as shown in Fig. 2. An ultrasonic sensor(USS) is used for obstacle recognition in the obstacle recognition system. 7 units USS are set every 20 degrees in front of cart, and it is recognized the height and the position of obstacle in front of the circumference of transportation object as shown in Fig.3, the obstacle information is heights data for transportation space segmented into$0.05^2 m^2$. In this research, the upper surface of the obstacle is assumed to be flat(as parallelepiped).

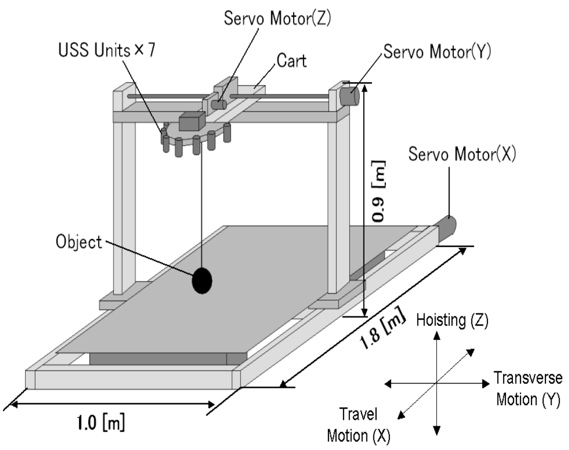

Figure 1: Experimental equipment.

3 PATH PLANNING SYSTEM

The three-dimensional path planning system for an overhead traveling crane proposed by our previous research is described in this section(kaneshige, 2012)(Nagai, 2011). Position relation of transportation object(T), obstacle(O), goal(G) is shown in Fig. 4. r_{fc} is a distance between transportation object and nearest obstacle to transportation object, and then **FC**(Feasible Circle) restricted transfer within a circle with the radius of r_{fc} is formed. In addition, **NP**(Next Position) is a position to transfer transportation object by calculation of once in **FC**. An equation derived **NP** is determined by expanding obstacle avoidance algorithm proposed by Srinivas to three-dimensional as follows (Kaneshige, 2012; Nagai, 2011).

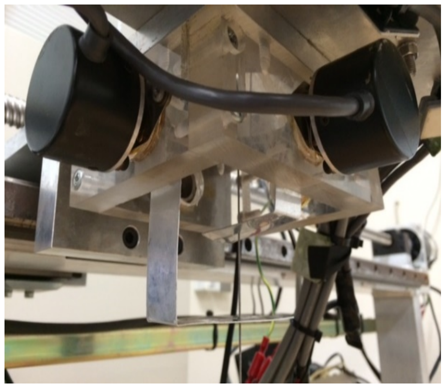

Figure 2: Measurement swing angle system.

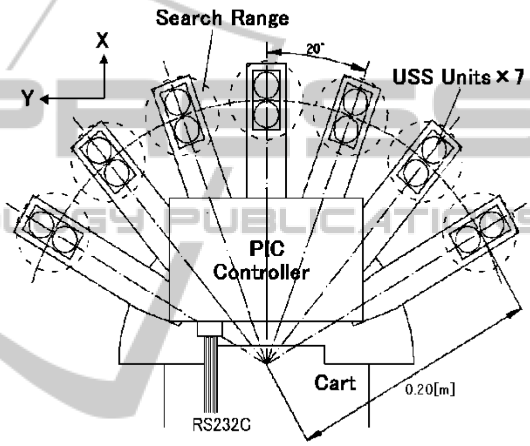

Figure 3: Ultra sonic sensor.

Objective function

$$F = (D_{gn})^2 - P_o \cdot (D_{on})^2 \quad (1)$$

Subject to the constraint

$$r_{fc}{}^2 = (x_n - x_t)^2 + (y_n - y_t)^2 + (z_n - z_t)^2 \quad (2)$$

Distance D_{gn} between goal and **NP** is shown in (3).

$$D_{gn} = \sqrt{(x_n - x_g)^2 + (y_n - y_g)^2 + (z_n - z_g)^2} \quad (3)$$

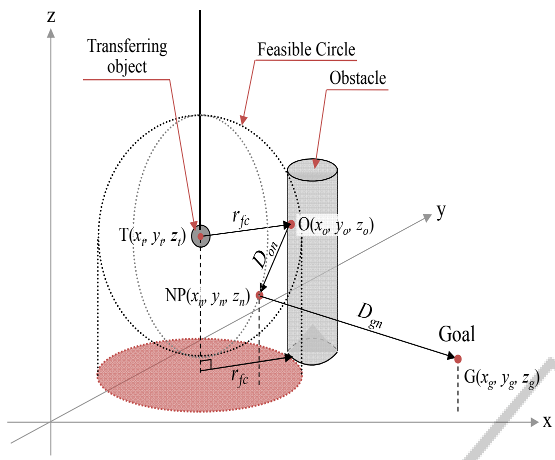

Figure 4: Position of each constituent in workspace.

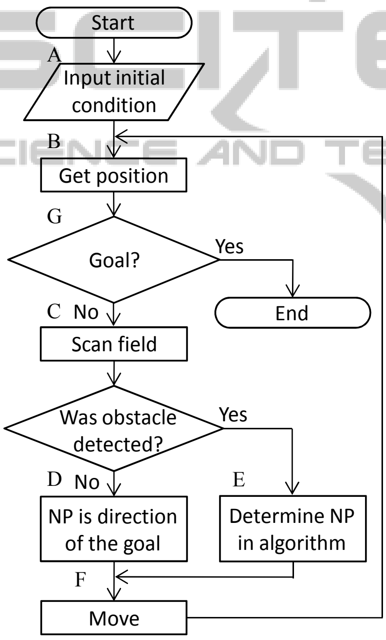

Figure 5: System flowchart.

Distance D_{on} between obstacle and **NP** is shown in (4).

$$D_{on} = \sqrt{(x_n - x_o)^2 + (y_n - y_o)^2 + (z_n - z_o)^2} \qquad (4)$$

(1) is minimized by Lagrange multiplier method. In addition, **NP** is derived by calculating minimized (1) and (2) at (x_n, y_n, z_n).

$$x_n = \{(x_g - x_t) - P_o(x_o - x_t) + C \cdot x_t\}/C \qquad (5)$$

$$y_n = \{(y_g - y_t) - P_o(y_o - y_t) + C \cdot y_t\}/C \qquad (6)$$

$$z_n = \{(z_g - z_t) - P_o(z_o - z_t) + C \cdot z_t\}/C \qquad (7)$$

where

$$C = \left\langle \begin{matrix} \{(x_g - x_t) - P_o(x_o - x_t)\}^2 + \{(y_g - y_t) - P_o(y_g - y_t)\}^2 \\ + \{(z_g - z_t) - P_o(z_g - z_t)^2\} \end{matrix} \right\rangle^{\frac{1}{2}} /(t_{fc} - t_r) \qquad (8)$$

NP is determined from (5), (6) and (7), therefore transportation object is transferred to **NP**. In addition, **NP** is determined from (5), (6) and (7) again when obstacle is recognized. This process is repeated until transportation object arrive at goal position. P_o of (1) is a value of weighting to adjust D_{gn} and D_{on}.

$$P_o = \frac{C_o}{D_{ot}} \qquad (9)$$

$$D_{ot} = \sqrt{(x_o - x_t)^2 + (y_o - y_t)^2 + (z_o - z_t)^2} \qquad (10)$$

D_{ot} is a distance between obstacle and transportation object. C_o of (9) is a optional coefficient to change size of avoidance path. Value of C_o is determined after evaluating C_o. Value of C_o is 300 by confirming in previous research (Kaneshige, 2012; Nagai, 2011).

Transportation path is generated by obstacle information, position information of goal position. Processing procedure flowchart of transportation path is shown in Fig. 5. Processing procedure is as follows.

A) Input initial condition of goal position and C_o
B) Get transportation object position.
C) Get obstacle information of circumference of transportation object from USS.
D) If obstacle is non-existent in range of detection of USS, **NP** is determined to transfer to direction of goal position.
E) If obstacle exist in range of detection of USS, **NP** is determined based on (5), (6) and (7).
F) Transportation object is transferred to **NP**.

Transportation is finished if transportation object position correspond with goal position when transportation object position is gotten again.

SCITEPRESS
SCIENCE AND TECHNOLOGY PUBLICATIONS

4 CONTROL SYSTEM OF SUPPRESSION OF LOAD SWING

The feed-forward control system using a notch filter is constructed in previous research(Kaneshige, 2012). However, the feed-forward control system was not able to control object swing which occurred during initial deviation or transportation. Therefore, in order to improve the vibration suppression of load swing, 2-degrees of freedom control system by using feed-forward control system and feed-back control system is constructed. Block diagram of control system is shown in Fig. 6.

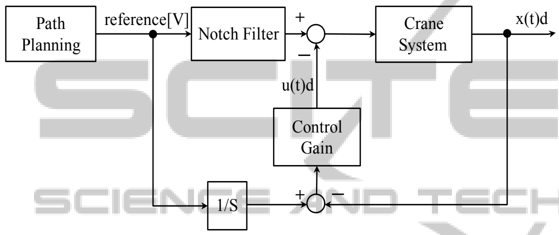

Figure 6: Constitution of the control system.

4.1 Generate Reference and Notch Filter

As for transportation control system, trapezoidal input voltage reference for speed control inputted each servo motor in X-direction and Y-direction is generated based on **NP** calculated by path planning system. In addition, transportation object is transferred to **NP** because input voltage reference applied notch filter is inputted to each servo motor. Natural frequency ingredient of input voltage reference is ridded by notch filter. Therefore, object swing is suppressed. Function of notch filter is shown in (11). ζ is damping ratio of object swing. ω_n is natural frequency of object swing.

$$G(s) = \frac{V_{out}(s)}{V_{in}(s)} = \frac{s^2 + 2\zeta\omega_n s + \omega_n^{\ 2}}{s^2 + \omega_n s + \omega_n^{\ 2}} \qquad (11)$$

4.2 Overhead Traveling Crane Model

In order to derive a feed-back gain used for feed-back control, state space model of overhead travelling crane is necessary. Therefore, the state space model is derived as shown in (12) and validity of the model is confirmed. Subscript d means a direction. x_t, y_t is cart position of each direction. x_n, y_n is reference trajectory input of each direction. α, β is object swing each angle. T_x, T_y is motor time constant of each direction. K_x, K_y is motor gain of each direction. D_x, D_y is object swing friction of each angle. L is rope length. However, rope length is constant because experimental equipment is small. Therefore, rope length is regarded linear time invariant. In addition, time variant control system for changing rope length is designed by previous research(Terashima, 1999). Each parameter value is shown in Table 1. The model is inspected by using MATLAB(Simulink). Further, cart position and object swing of experimental equipment is compared when input voltage reference similar to simulation is inputted. Comparison result of cart position is shown in Fig. 7(a). Comparison result of object swing is shown in Fig. 7(b). As shown from Fig. 7, simulation and experimental equipment described mostly the same line both cart position and object swing. Therefore, validity of derived model of overhead crane is confirmed.

$$\left.\begin{aligned}
&\dot{x}(t)_d = A_d(t)_d + B_d(t)_d \\
&y(t)_d = C_d x(t)_d \\
&A_d = \begin{bmatrix} 0 & 1 & 0 & 0 \\ 0 & -\frac{1}{T_d} & 0 & 0 \\ 0 & 0 & 0 & 1 \\ 0 & -\frac{1}{T_d L} & -\frac{g}{L} & -\frac{D_d}{mL^2} \end{bmatrix} \\
&B_d = \begin{bmatrix} 0 \\ \frac{1}{T_d} \\ 0 \\ \frac{K_d}{T_d L} \end{bmatrix} C_d = \begin{bmatrix} 1 & 0 & 0 & 0 \\ 0 & 1 & 0 & 0 \\ 0 & 0 & 1 & 0 \\ 0 & 0 & 0 & 1 \end{bmatrix} \\
&x_x = \left[x_r - x_t, \dot{x}_r - \dot{x}_t, \alpha, \dot{\alpha}\right]^T \\
&x_y = \left[y_r - y_t, \dot{y}_r - \dot{y}_t, \beta, \dot{\beta}\right]^T
\end{aligned}\right\} \qquad (12)$$

Table 1: Parameter of overhead crane.

	X	Y
Motor Gain [m/s・V]	0.2242	0.1118
Motor Time Constant	0.01	0.01
Shake Friction Coefficient[kg/s]	10^{-7}	10^{-7}
Rope length [m]	0.65	0.65

SCITEPRESS SCIENCE AND TECHNOLOGY PUBLICATIONS

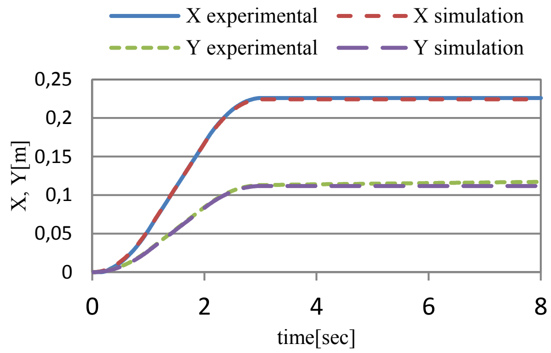

(a) Cart position

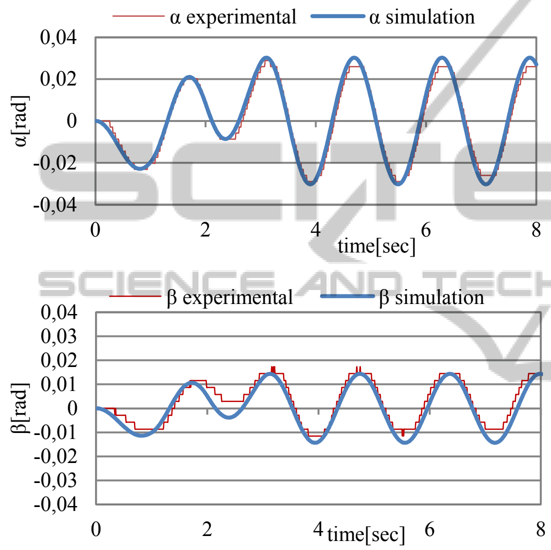

(b) Swing angle

Figure 7: Validation of crane model.

4.3 Construction of Feed-Back Control System

A control system of each X-direction and Y-direction is constructed independently. A control system of Z-direction isn't constructed because it is guaranteed regardless of object swing. As for constructed control system, notch filter is applied to value of input voltage reference derived by path planning system, and feed-back gain is applied to deflection between reference position and transportation object position($x_r - x_t$, $y_r - y_t$), deflection between reference speed and transportation object speed($\dot{x}_r - \dot{x}_t$, $\dot{y}_r - \dot{y}_t$), object swing(α , β) and object swing speed($\dot{\alpha}$, $\dot{\beta}$). Therefore, suppression of object swing is conducted by comparing these values. Based on confirmed overhead crane model, Feed-back gain is derived by using optimal regulator. An optimum control input due to state feed-back is determined by minimizing evaluation function as shown in (13).

$$J = \int_0^\infty [x^T Q x + u^T R u] dt \tag{13}$$

$$u = -Fx \tag{14}$$

Feed-back gain is derived by deciding value of Q and R with trial and error.

4.4 Feed-back Gain

How to determine the feed-back gain an explained in this section. In this research, feed-back gain are determined by comparing the suppression of object oscillating and the conformity to the reference trajectory. Feed-back gain are determined by which is setting the weight of R and Q as follows.

Case1: In case of considering the suppression of objects oscillation

$$Q = \begin{bmatrix} 10 & 0 & 0 & 0 \\ 0 & 0.01 & 0 & 0 \\ 0 & 0 & 200 & 0 \\ 0 & 0 & 0 & 0.01 \end{bmatrix}, R = 1$$

$$F_x = [3.1623 \quad 1.1746 \quad 13.9871 \quad 0.5470]$$
$$F_y = [3.1623 \quad 0.7775 \quad 13.7073 \quad 0.9018]$$

Case2: In case of considering the conformity to the reference trajectory

$$Q = \begin{bmatrix} 500 & 0 & 0 & 0 \\ 0 & 0.01 & 0 & 0 \\ 0 & 0 & 20 & 0 \\ 0 & 0 & 0 & 0.01 \end{bmatrix}, R = 1$$

$$F_x = [22.3607 \quad 3.1368 \quad 3.9146 \quad -1.5658]$$
$$F_y = [22.3607 \quad 2.8927 \quad 4.4057 \quad -0.2216]$$

Comparison between reference trajectory generated by path planning system and transportation path(experimental results) each feed-back gain is shown in Fig. 8(a)(b). X-direction object swing of each case are shown in Fig. 9(a)(b). Y-direction object swing of each case are shown in Fig. 10(a)(b). Comparison of transportation time is shown in Table 2. As for transportation result, comparison is made due to X-Y surface because control system of Z-direction isn't constructed.

As shown from Fig. 8(a)(b), it can be seen that the transportation path of case 2, as compared with case 1, is conformed to the reference trajectory. As

SCITEPRESS SCIENCE AND TECHNOLOGY PUBLICATIONS

shown from Fig. 9(a)(b), it can be seen that case 1 suppresses object swing a little as compared with case 2. However, both of them suppress object swing to some extent. As shown from fig. 10(a)(b), it can be seen same as Fig 9(a)(b). As shown from Table 2, it can be seen that transportation time of case 2 is shorter than case 1. From the above results, it seems that case 2 is more effective than case 1 because the transportation path is conformed to the reference trajectory, transportation time is shorter and object swing is suppressed to some extent.

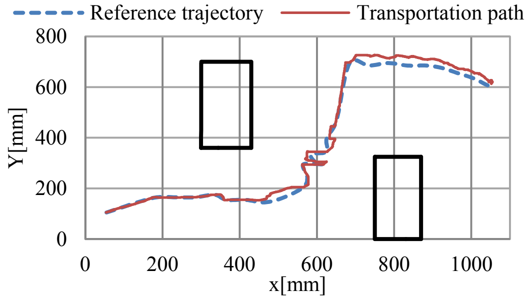

Figure 8(a): experimental result of path (case 1).

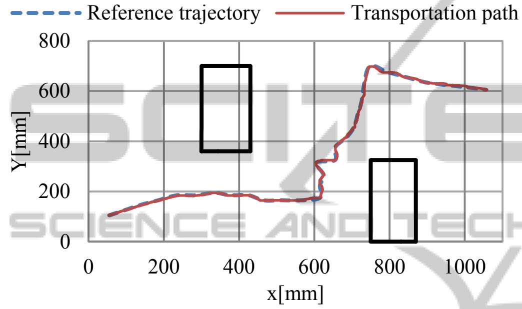

Figure 8(b): experimental result of path (case 2).

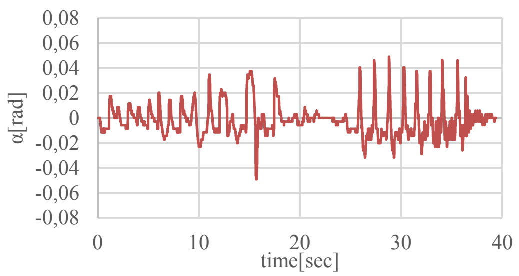

Figure 9(a): X-direction object swing (case 1).

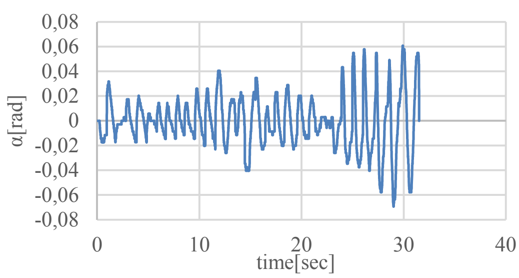

Figure 9(b): X-direction object swing (case 2).

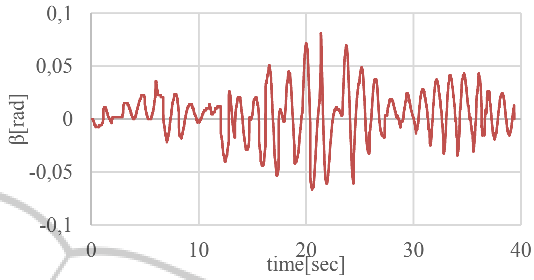

Figure 10(a): Y-direction object swing(Case 1).

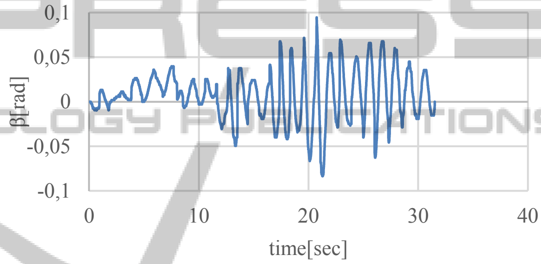

Figure 10(b): Y-direction object swing(Case 2).

Table 2: Comparison of transportation time.

	Transportation time
Case 1	39.38sec
Case 2	31.58sec

5 TRANSPORTATION EXPERIMENT

Two-degrees of freedom control system by feed-back gain derived in section 4.4 and notch filter are implemented in control computer. In addition, transportation experiment is conducted. Experimental results of two-degrees of freedom control system are compared against experimental results of feed-forward control system, and then usefulness of control system constructed is confirmed.

5.1 Experiment Condition

Transferring space of X-direction is 1.2[m], Y-direction is 0.75[m], and Z-direction is 0.35[m] by

SCITEPRESS SCIENCE AND TECHNOLOGY PUBLICATIONS

experimental equipment of overhead crane. Two obstacles are disposed between start position S(50,

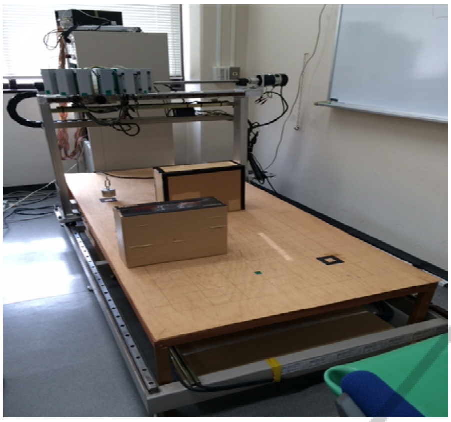

Figure 11: Placement of obstacles.

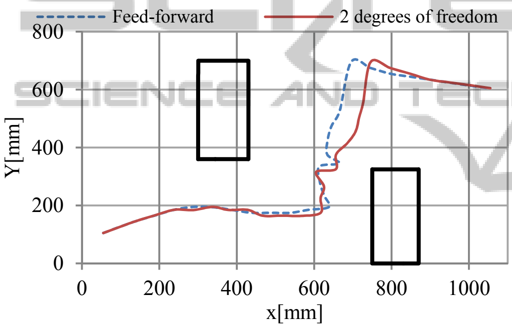

Figure 12(a): Experimental result of path(X-Y surface).

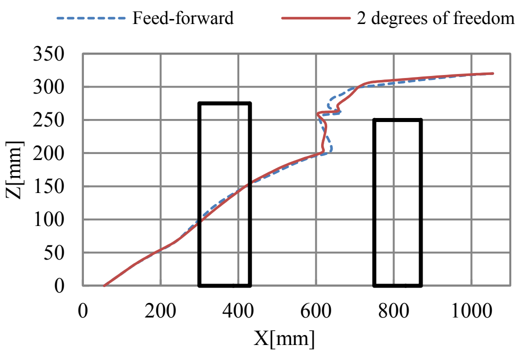

Figure 12(b): Experimental result of path(X-Z surface).

100, 0) and goal position G(1050, 650, 320) as shown in Fig. 11. It is assumed that transportation object avoid obstacles and transportation object reach for goal position. Transportation object is used a column of 1.0kg in weight, 50mm in radius, and 30mm in height. Placement of obstacles are shown in Fig. 11

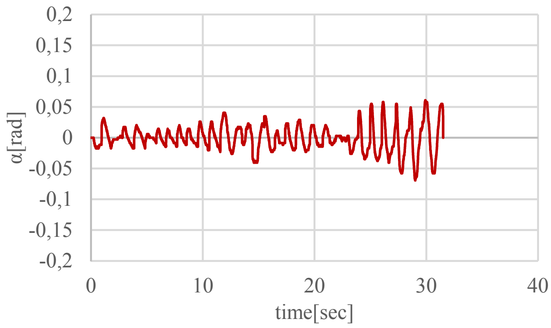

Figure 13(a): X-direction object swing(2 degrees of freedom).

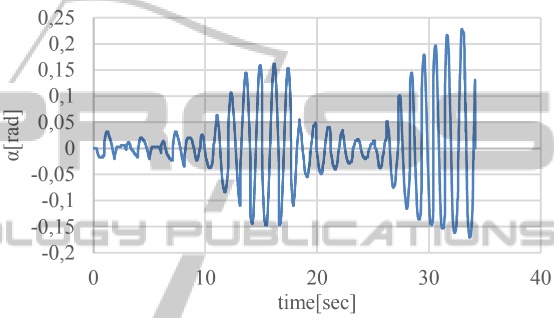

Figure 13(b): X-direction object swing(Feed-forward).

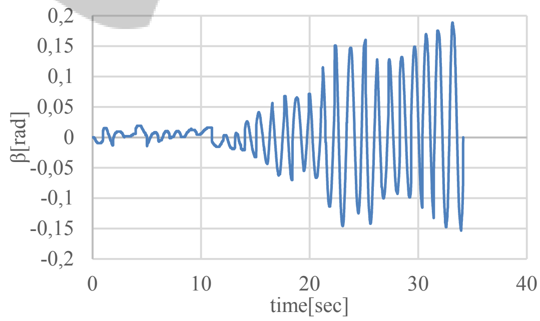

Figure 14(a): Y-direction object swing(2 degrees of freedom).

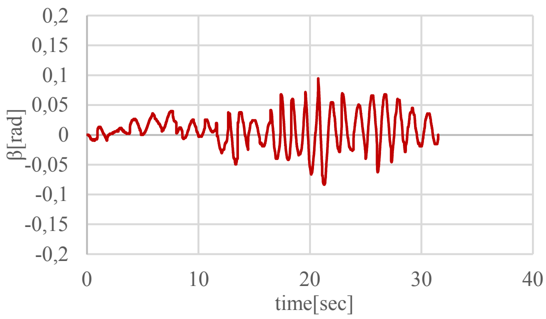

Figure 14(b): Y-direction object swing (Feed-forward).

SCITEPRESS SCIENCE AND TECHNOLOGY PUBLICATIONS

Table 3: Experimental value.

	transportation time
Feed-forward	34.19sec
Two-degrees of freedom	31.51sec

5.2 Experimental Results

Comparison of transportation path(X-Z surface, X-Y surface) is shown in Fig. 12(a)(b), X-direction object swing of each case are shown in Fig. 13 (a)(b), Y-direction object swing of each case are shown in Fig. 14(a)(b), and transportation time is shown in Table 3. As shown from Fig. 12(a)(b), change of transportation path is occurred a little because feed-back control system is used. However, both of transportation paths are almost the same, therefore it can be said that suitable transportation is conducted because transportation object is avoided obstacles from start position to goal position. As shown from Fig. 13(a)(b), Fig. 14(a)(b) and Table 3, transportation time of two-degrees of freedom control system is shorter than feed-forward control system. In addition, object swing of two-degrees of freedom control system is less than feed-forward control system. Therefore, the usefulness of constructed transportation control system is confirmed through experiments.

6 CONCLUSIONS

The conclusion in this research for an autonomous mobile crane system can be summarized as follows.

- The on-line obstacle recognition system using an USS and the on-line obstacle avoidance path planning system is constructed.
- Based on system integrated, the transportation control system to suppress a object swing is constructed by using two-degrees of freedom control system
- Feed-back gain considering the suppresion of object oscillation and the conformity to the reference trajectory are determined, and then it is confirmed by experiment.
- The usefulness of constructed transportation control system is confirmed through experiments.

REFERENCES

A. Kaneshige, et al.: 2012-9. Development of the Autonomous Overhead Travelling Crane with Real Time Path-Planning Based on Obstacle Information, *Proc. of 13th IFAC Symposium on Control in Transportation Systems CTS'2012* Sofia (Bulgaria), Sept.12-14, 2012, pp.274/279.

S. Nagai, A. Kaneshige and S. Ueki: 2011-8. Three-Dimensional Obstacle Avoidance Online Path-Planning Method for Autonomous Mobile Overhead Crane, *Proc. of the 2011 IEEE IEEE/ASME International Conference on Mechatronics and Automation*, Beijing(China), CD-ROM, pp.1497/1502.

K. Terashima and A. Kaneshige: 1999. Load-Position Control of Overhead travelling crane in terms of Fixed-Pole App.roach for 3-D Trasfer Path, Proc.of the European Control ECC'99, Karlsruhe, Geramany, Aug-Sep. BP11.

Y. L. Srinivas and S. N. Kramer, 1991. An Algorithm For Real-Time Obstacle Avoidance A *Conference a*nd Path Planning For Mobile Robots, Advances in Design Automation, **2**, 507-514.

SCIENCE AND TECHNOLOGY PUBLICATIONS